

Eddy growth and mixing in mesoscale oceanographic flows

G. Haller and A. C. Poje

Division of Applied Mathematics, Brown University, Providence, Rhode Island, USA

Received: 17 May 1997 – Accepted: 3 July 1998

Abstract. We study the relation between changes in the Eulerian topology of a two dimensional flow and the mixing of fluid particles between qualitatively different regions of the flow. In general time dependent flows, streamlines and particle paths are unrelated. However, for many mesoscale oceanographic features such as detaching rings and meandering jets, the rate at which the Eulerian structures evolve is considerably slower than typical advection speeds of Lagrangian tracers. In this note we show that for two-dimensional, *adiabatic* fluid flows there is a direct relationship between observable changes in the topology of the Eulerian field and the rate of transport of fluid particles. We show that a certain class of flows is amenable to adiabatic or near adiabatic analysis, and, as an example, we use our results to study the chaotic mixing in the Dutkiewicz and Paldor (1994) kinematic model of the interaction of a meandering barotropic jet with a strong eddy.

meandering jets (Samelson, 1991) and numerical simulations of quasi-geostrophic jets (Lozier et al., 1997).

While the Lagrangian, dynamical systems viewpoint is a powerful tool for the study of particle dynamics, in many applications one hopes to deduce the nature and degree of particle mixing from the motion of *coherent structures* in the Eulerian frame. A classic oceanographic example is the estimate of Lagrangian particle fluxes from intermittent observations of Eulerian data, sea surface height or temperature, provided by satellites. The simplest classification of these structures is to lump them into either of two categories; those with open streamlines, *jets*, and those with closed streamlines *eddies* (see, e.g., Wray and Hunt (1990)). Nondegenerate contour plots are built of eddies and jets as well as critical contour lines that separate the jets and the eddies. These plots deform in time and often exhibit qualitative changes or “catastrophic events”, such as the creation and disappearance of eddies, detachment of a ring from a jet, merger of eddies, etc. We will refer to such events as *Eulerian bifurcations*.

1 Introduction

For two dimensional, incompressible flows, the equations describing the the time evolution of Lagrangian particle trajectories are exactly those of a Hamiltonian system where the *phase space* of the dynamical system is precisely the physical space of the flow. This formulation of the Lagrangian problem, pointed out by Aref (1984), allows one to apply the geometric techniques of dynamical systems theory (see for example MacKay et al. (1984), Rom-Kedar et al. (1990), Wiggins (1992)) to determine particle (or “phase space volume”) flux with respect to surfaces separating regions of different kinematic behavior (i.e. the interior/exterior of a ring or eddy). Studies of such ‘chaotic mixing’ have been conducted for a variety of oceanographic flows including tidal basins (Ridderinkhof and Zimmerman, 1992), kinematic models of

Our main goal in this paper is to provide a rigorous, mathematical relationship between topological changes in an Eulerian field and Lagrangian particle mixing. We would like to know precisely when and how observed bifurcations in the topology of the Eulerian velocity field indicate chaotic transport in the Lagrangian dynamics. Obviously, since particle pathlines and instantaneous streamlines are not coincident in a time dependent flow, there exists no general relationship between changes in Eulerian topography and chaotic mixing of Lagrangian particles. However, observational evidence indicates that in many geophysical situations, the temporal evolution of mesoscale structures occurs on time scales which are slow compared to typical particle speeds (see Holdzkom et. al. (1995) for one particular example). In such *adiabatic* cases, particle paths and streamlines are correlated over significant lengths of time and it is possible to establish a relationship between defor-

mations of the Eulerian field and Lagrangian mixing.

We begin this study by defining Eulerian bifurcations in geometric terms for two-dimensional, incompressible flows. Throughout, we make use of the non-divergent nature of the two-dimensional flow, hence our results are strictly applicable in the quasi-geostrophic limit. Loosely speaking, we define an Eulerian bifurcation within a bounded region as a change in the number of connected components of a level curve of the streamfunction. In the generic case, such a change is manifested by eddy creation, eddy disappearance, eddy detachment, or eddy reattachment. While there is a substantial body of literature on eddy formation especially in the context of oceanographic jets, (see, e.g., Pratt and Stern (1986), Feliks and Ghil (1996), and the references cited therein), Theorem 2.1 provides a useful dynamic means of classifying eddy formation, disappearance, detachment, and reattachment in terms of the eigenspace of frozen time stagnation points.

In Section 3 we focus on adiabatic flow fields. We state a readily observable geometric condition for the presence of Lagrangian mixing: *Increasing detached eddies or shrinking reattaching eddies imply transport of fluid particles in directions transverse to the eddy boundary.* Using a result due to Kaper and Kovačič (1994), we are also able to predict the corresponding Lagrangian flux directly from Eulerian observations if the flow is time-periodic.

As an example of the application of the theorems, we study a kinematic model of eddy-jet interaction (Dutkiewicz and Paldor, 1994) in Section 4. For the case of strong eddies, where the controlling saddle type fixed point exists for all times, we use the results from Section 2 to predict the occurrence of eddy detachment and reattachment in space and time. We also use the eddy growth criterion to show the presence of chaotic Lagrangian transport of particles between the jet and the eddy. We close the paper with conclusions and remarks about general, aperiodic time dependence in Section 5.

2 The geometry of Eulerian bifurcations

The velocity field of a two-dimensional, incompressible fluid satisfies the equation

$$\begin{aligned} v_x &= \frac{\partial \psi(x, y, t)}{\partial y}, \\ v_y &= -\frac{\partial \psi(x, y, t)}{\partial x}, \end{aligned}$$

where the smooth streamfunction ψ is a time-dependent Hamiltonian for particle motions. To eliminate the inherent non-uniqueness in the definition of ψ for a given flow, we assume that ψ contains no spatially independent additive terms. At any point in time, particle velocities are tangent to the instantaneous streamlines, i.e., the level curves of ψ . In the analysis of experimental or

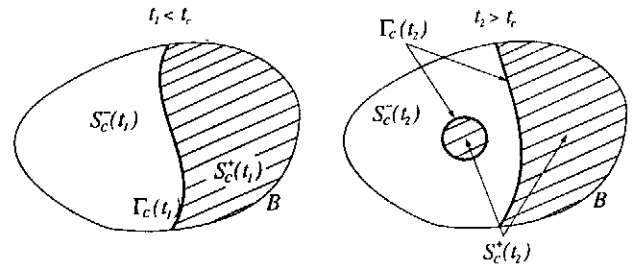


Fig. 1. The main concept of Eulerian bifurcations.

numerical data, one typically follows the evolution of a set of streamlines whose associated ψ -values fall in the range of interest. For this reason, we develop the concept of Eulerian bifurcations based on the geometry of streamlines. However, a similar treatment can be given for other Eulerian fields, such as temperature, density, etc.

Let us fix a bounded, open, and connected set $B \subset \mathcal{R}^2$ in the physical space of particle motions. Let us also fix a number $c \in \mathcal{R}$, and for any time t define the two open sets

$$\begin{aligned} S_c^+(t) &= \{(x, y) \in B \mid \psi(x, y, t) > c\}, \\ S_c^-(t) &= \{(x, y) \in B \mid \psi(x, y, t) < c\}. \end{aligned}$$

The dividing line between the two sets is given by the time-dependent curve

$$\Gamma_c(t) = \partial S_c^+(t) = \{(x, y) \in B \mid \psi(x, y, t) = c\}.$$

Note that $S_c^+(t)$, $S_c^-(t)$, and $\Gamma_c(t)$ give a partition of B for any t , including the possibility of a trivial partition when only $S_c^+(t)$ or $S_c^-(t)$ is nonempty. Also note a geometric interpretation of $\Gamma_c(t)$ in the extended phase space of the (x, y, t) variables: $\Gamma_c(\tau)$ is the intersection of the plane $t = \tau$ with the two-dimensional surface $\psi(x, y, t) = c$.

We could color the streamlines with $\psi > c$ with darker colors and those with $\psi < c$ with lighter colors. Intuitively, a change in coherent structures would mean the mixing of these two colors, e.g., the penetration a blob of dark colors into a region that was originally occupied fully by light colors (see Fig. 1) In the extended phase space of the variables x, y , and t , such an event is manifested by the folding and splitting of the surface $\psi(x, y, t) = c$ (see Fig. 2). Our definition below puts this intuitive notion of Eulerian bifurcation into a mathematical framework.

Let $N_c(t)$ denote the number of connected components of the dividing curve $\Gamma_c(t)$. In the following we will be interested in cases when both $S_c^+(t)$ and $S_c^-(t)$,

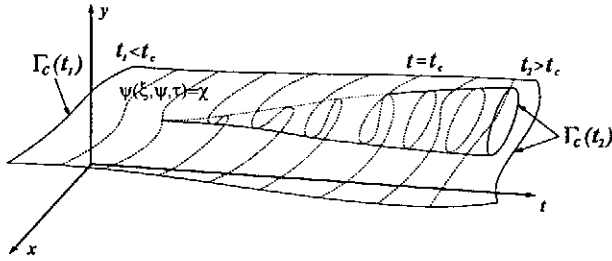


Fig. 2. The manifestation of an Eulerian bifurcation in the extended phase space.

and hence $\Gamma_c(t)$ are nonempty on the same time interval. Note that $N_c(t)$ is a well-defined, finite, nonzero integer for any $t \in [t_0, t_1]$.

Definition 2.1 We say that an Eulerian bifurcation of the streamline $\psi = c$ occurs at $t = t^* \in (t_0, t_1)$ in B , if the value of N_c changes at t^* , i.e., the function $N_c(t)$ has a discontinuity at $t = t^*$.

Hence, by an Eulerian bifurcation we mean a change in the topology of the two regions $S_c^+(t)$ and $S_c^-(t)$, since at least one of them gains a connected component if the value of N_c increases, or loses a connected component when N_c decreases. As we will see below, this connected component is typically an eddy, i.e., a closed contour curve of the streamfunction ψ .

If the gradient

$$\nabla\psi(x, y, t_0) = (\partial\psi(x, y, t_0)/\partial x, \partial\psi(x, y, t_0)/\partial y)$$

is nonzero restricted to $\Gamma_c(t_0)$, then $\Gamma_c(t_0)$ is a smooth curve by the implicit function theorem. Hence $\Gamma_c(t_0)$ locally divides the set B into two open regions, one of which is characterized by streamfunction values above c and the other is by values below c . By the continuity of $\nabla\psi$ in t , this distinction between the two sides of Γ_c persists for times close to t_0 . Hence although the connected components of the curve $\Gamma_c(t)$ in general move in time, the two regions $S_c^+(t)$ and $S_c^-(t)$ remain locally separated, and the value of $N_c(t)$ is constant. As a result, no Eulerian bifurcation occurs.

For some larger value $t = t_c$, however, we may have a point $p_c = (x_c, y_c) \in \Gamma_c(t_c)$, such that

$$\nabla\psi(x_c, y_c, t_c) = 0 \tag{1}$$

holds. In the generic case, we can assume that this event occurs under the nondegeneracy conditions

$$\det \begin{bmatrix} \frac{\partial^2 \psi}{\partial x \partial y} \Big|_{(x_c, y_c, t_c)} \\ \frac{\partial \psi}{\partial t} \Big|_{(x_c, y_c, t_c)} \end{bmatrix} \neq 0, \tag{2}$$

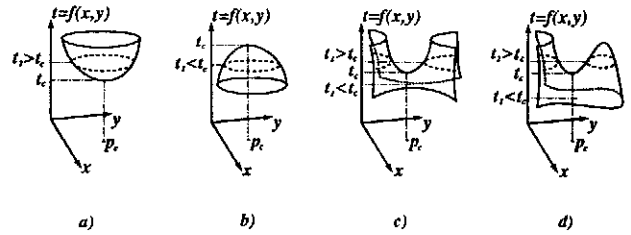


Fig. 3. Nondegenerate critical points for the streamfunction and Eulerian bifurcations.

The first condition implies that at the point p_c , the function $\psi(x, y, t_c)$ has either a local minimum, a local maximum, or a saddle point. The second condition means that the value of the streamfunction changes in time at the point p_c . It allows us to express the variable t on the surface $\psi = c$ as a function, f , of (x, y) near (x_c, y_c, t_c) in the extended phase space. The function $t = f(x, y)$ also has a local extremum at p_c , since by implicit differentiation we obtain

$$\begin{aligned} \nabla f(x_c, y_c) &= -\frac{\nabla\psi(x_c, y_c, t_c)}{\frac{\partial}{\partial t}\psi(x_c, y_c, t_c)}, \tag{3} \\ \frac{\partial^2}{\partial x \partial y} f(x_c, y_c) &= -\frac{\frac{\partial^2}{\partial x \partial y}\psi(x_c, y_c, t_c)}{\frac{\partial}{\partial t}\psi(x_c, y_c, t_c)}. \end{aligned}$$

Note that the level curves $f(x, y) = t$ coincide with the level curves $\psi(x, y, t) = c$ near p_c , for times close to t_c .

Suppose now that f has a local minimum at p_c (see Fig. 3a). Then a connected component of $\Gamma_c(t_c)$ will turn from the point p_c into a smooth closed curve as time increases. This event increases the number $N_c(t)$ by one for $t > t_c$. If p_c is a point of local maximum for f , then the corresponding component of $\Gamma_c(t)$ will be a closed curve that shrinks to the point p_c and then disappears (see Fig. 3b). Hence, this event will decrease the number $N_c(t)$ by one at $t = t_c$. Finally, if f has a saddle point at p_c , then $\Gamma_c(t)$ undergoes a self-intersection and a metamorphosis at p_c . This event may or may not change the number of connected components of Γ_c . The number remains unchanged if neither of the colliding components of Γ_c is a closed curve. This case is a simple “exchange of streamlines”, as shown in Fig. 3c. However, N_c changes if one of the two interacting components is a closed streamline, either before or after the collision, as shown in Fig. 3d. Equivalently, N_c changes at $t = t_c$ if $\Gamma_c(t_c)$ contains a closed loop attached to the point p_c . This will certainly be the case if $\Gamma_c(t_c)$ intersects the boundary ∂B of the domain B at no more than two points.

The above discussion shows that in the generic case, an Eulerian bifurcation is manifested by a creation, dis-

appearance, detachment, or reattachment of closed streamlines, i.e., *eddies*. Using the formulas in (3), and the matrix

$$E(p_c, t_c) = \frac{\partial}{\partial t} \psi(x_c, y_c, t_c) \cdot \frac{\partial^2}{\partial x \partial y} \psi(x_c, y_c, t_c), \quad (4)$$

we can summarize our discussion as follows.

Theorem 2.1 *Suppose that the streamline $\Gamma_c(t)$ intersects the boundary of B in precisely two points for all $t \in [t_0, t_1]$. Assume further that there exists a time t_c in the interval and a point $p_c = (x_c, y_c) \in \Gamma_c(t_c)$ such that $\nabla \psi(x_c, y_c, t_c) = 0$ and the matrix $E(p_c, t_c)$ defined in (4) is nonsingular. Then an Eulerian bifurcation of the streamline $\psi = c$ occurs at time $t = t_c$. The bifurcation is an*

- a) eddy creation if $E(p_c, t_c)$ is negative definite,
- b) eddy disappearance if $E(p_c, t_c)$ is positive definite,
- c) eddy detachment or reattachment if $E(p_c, t_c)$ is indefinite, i.e., it has a strictly positive and a strictly negative eigenvalue.

If an Eulerian bifurcation satisfies the nondegeneracy condition of Theorem 2.1, then we call it a *nondegenerate Eulerian bifurcation*.

We now make several remarks in order:

1.. Eulerian bifurcations of streamlines are not isolated events: they also occur on nearby streamlines at some nearby times. This follows from the fact that equation (1) can locally be solved for values of t close to t_c , which is guaranteed by the first nondegeneracy condition in (2) and the implicit function theorem. The solution is a one-parameter family of points $(x_c(t), y_c(t)) = (x_c, y_c) + \mathcal{O}(t - t_c)$, which gives the location of nondegenerate critical points on nearby streamlines for times close to t_c . By the continuity of the matrix E in p_c and t_c , this means that the same type of Eulerian bifurcation occurs on nearby streamlines at nearby times.

2.. Eddy creation and disappearance are “discontinuous” events, as eddies from region S_c^+ get mixed into region S_c^- (or vice versa) without crossing the boundary between the two regions. By the same token, eddy detachment or reattachment are *continuous* events. We will refer to such an event as a *continuous Eulerian bifurcation*.

3.. Since eddy detachment or reattachment always happens through the formation of a closed loop in a streamline, in such cases the Hamiltonian system generated by $\psi(x, y, t_c)$ necessarily has a homoclinic or heteroclinic orbit attached to the saddle point p_c . Hence the region B can always be picked in a way that its boundary is intersected at precisely two points by the components of the stable and unstable manifold of the saddle-point p_c , but is *not* intersected by the homoclinic loop of interest. Thus the intersection condition of Theorem 2.1 can be replaced by the condition that the Hamiltonian $\psi(x, y, t_c)$ has a homoclinic or heteroclinic orbit attached to the point p_c . One can use the intersection condition if the details of the contour plot of $\psi(x, y, t_c)$ are not exactly known, e.g., when the vector field is numerically generated. In such a case one only has to check through the boundary of a suitable domain B to find the number of points at which the streamfunction takes the value c . By the continuity of ψ , this algorithm is robust with respect to numerical errors.

4.. In the case of eddy creation or disappearance, the point p_c is a center-type fixed point for the Hamiltonian $\psi(x, y, t_c)$.

5.. We note that while the above bifurcation results are applicable to any Eulerian scalar field, $f(x, y, t)$, passively advected fields violate the nondegeneracy conditions (1) and (2) by definition. The advection equation,

$$\frac{\partial f}{\partial t} + \mathbf{v} \cdot \nabla f = 0,$$

implies that for a general velocity field \mathbf{v} , the time derivative of the scalar is identically zero when the gradient is zero. This implies that topological changes of the type classified here require dissipative effects, however small, in the governing PDEs.

3 Adiabatic flows

Adiabatic flows are governed by velocity fields whose explicit time-dependence is slow. Such flows are relevant models for various mesoscale geophysical situations where the speeds of pertinent Eulerian structures are significantly slower than representative particle speeds. For example, the phase speed of Gulf Stream meanders (Song et al., 1995) and the modulation frequency of warm core rings (Holdzkom et al., 1995) are believed to be small compared to the advection speeds of particles contained in these structures.

Adiabatic velocity fields derive from streamfunctions of the form $\psi(x, y, \epsilon t)$, where ϵ is a small parameter. Introducing the variable $z = \epsilon t$, one can describe the dynamics of the particles by a three-dimensional, autonomous system of the form

$$\begin{aligned} \dot{x} &= -\frac{\partial \psi(x, y, z)}{\partial y}, \\ \dot{y} &= \frac{\partial \psi(x, y, z)}{\partial x}, \\ \dot{z} &= \epsilon. \end{aligned} \quad (5)$$

This system has the important feature that for $\epsilon = 0$, the variable z is an integral. Hence, in the adiabatic limit the particle motions indeed follow the level curves of $\psi(x, y, z)$ with z fixed. (Note that in general, the fictitious particle motions generated by $(\dot{x}, \dot{y}) = (-\psi_x(x, y, t_0), \psi_y(x, y, t_0))$ are unrelated to the true particle motions governed by $(\dot{x}, \dot{y}) = (-\psi_x(x, y, t), \psi_y(x, y, t))$.) This fact distinguishes adiabatic systems from the point of view of transport, because the deviation of particles from streamlines only occurs on long times scales.

For Lagrangian mixing to take place for $\epsilon > 0$ small, we need the existence of qualitatively different regions for the $\epsilon = 0$ limit of system (5). This can be assured by assuming the existence of a saddle point $p(z) = (x_p(z), y_p(z))$ with a homoclinic solution $\gamma^h(t; z) = (x^h(t; z), y^h(t; z))$ for the first two equations in (5) for a range of z values, say $z \in [z^-, z^+]$. Then for $\epsilon = 0$, the two-dimensional homoclinic manifold

$$\Gamma_0 = \{(x, y, z) \mid \exists t \in \mathcal{R}: x = x^h(t; z), y = y^h(t; z)\}$$

divides the three-dimensional phase space of (5) into a simply and a doubly connected region with qualitatively different solutions. Γ_0 connects the set

$$P_0 = \{(x, y, z) \mid x = x_p(z), y = y_p(z), z \in [z^-, z^+]\}$$

to itself. P_0 clearly admits two dimensional stable and unstable manifolds $W^s(P_0) \equiv W^u(P_0) \equiv \Gamma_0$. P_0 is a one-dimensional, normally hyperbolic invariant manifold, hence it perturbs to a nearby, locally invariant manifold P_ϵ for $\epsilon > 0$ small (Fenichel, 1971). Local invariance means that solutions starting on P_ϵ can leave the manifold only through its boundary. Ultimately, all solutions will leave P_ϵ in both forward and backward time since $\dot{z} = \epsilon \neq 0$, i.e., P_ϵ is a compact piece of a single slow solution. As shown by Wiggins (1987) (see also Wiggins (1987)), the persisting (locally invariant) stable and unstable manifolds $W^u(P_\epsilon)$ and $W^s(P_\epsilon)$ intersect each other transversely if the Melnikov function

$$M(z) = \int_{-\infty}^{+\infty} \left[\frac{\partial \psi}{\partial z}(\gamma^h(t; z), z) - \frac{\partial \psi}{\partial z}(p(z), z) \right] dt \quad (6)$$

has a transverse zero z_0 which falls in the range $[z_-, z_+]$. Each transverse zero of this function indicates a different solution which has a compact piece in $W^u(P_\epsilon) \cap W^s(P_\epsilon)$. Kaper and Kovačič (1994) found the following relationship between the Melnikov function and the area $A(z)$ enclosed by the unperturbed homoclinic solution $\gamma^h(t; z)$:

$$M(z) = \frac{dA(z)}{dz}. \quad (7)$$

This formula means that each nondegenerate local extremum of the area function $A(z)$ (see Fig. 4) gives rise to a transverse zero of $M(z)$.

If the function $M(z)$ has at least two transverse zeros $z_1, z_2 \in [z^-, z^+]$, then at least one *three-dimensional lobe* (*three-lobe*) is formed by the intersecting manifolds. This lobe is the volume enclosed by the subsets of the stable and unstable manifolds that are bounded by two intersection orbits, as shown in Fig. 5. By the invariance of $W^u(P_\epsilon)$ and $W^s(P_\epsilon)$, the three-lobe is a locally invariant set. Once such a lobe is present, it provides a “channel” through which a solution $\gamma(t)$ can travel from the exterior of the homoclinic manifold Γ_0 to its interior (see Fig. 5). Therefore, *Lagrangian transport of initial conditions* occurs whenever $M(z)$ has at least two, distinct, transverse zeros.

By the area-preserving nature of the flow map $(x_0, y_0) \mapsto (x(t; x_0), y(t; x_0))$, the intersections of the three-lobe with $z = z_0 = \epsilon t_0$ surfaces has the same area for all $z_0 \in [z^-, z^+]$ (see Fig. 5). The intersection of the three-lobe with these constant time surfaces gives two-dimensional lobes (two-lobes), as seen from Fig. 5. Kaper and Kovačič showed (see also Kaper and Wiggins (1991)) that the area A_L of the two-lobe obeys the formula

$$A_L = \int_{z_1}^{z_2} M(z) dz + \mathcal{O}(\epsilon) = A(z_2) - A(z_1) + \mathcal{O}(\epsilon), \quad (8)$$

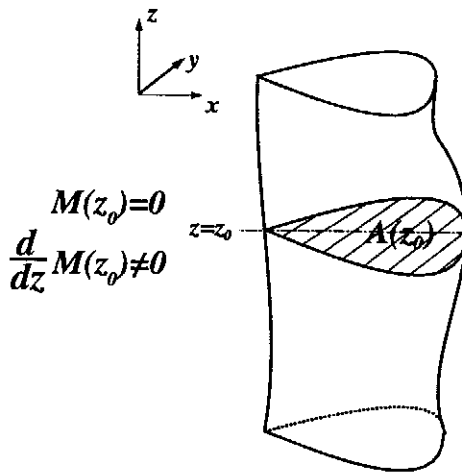


Fig. 4. Relationship between the geometry of the homoclinic manifold and transverse zeros of the Melnikov function.

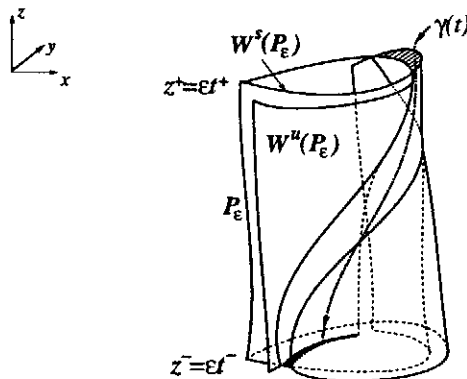


Fig. 5. Lagrangian transport through a three-dimensional lobe.

where z_1 and z_2 are adjacent transverse zeros of the Melnikov function. Note that the two-lobe area is of order $\mathcal{O}(1)$, which is due to the singular perturbation nature of adiabatic problems. *All facts about lobes that we have discussed so far remain valid even if z_1 and z_2 are only topologically transverse zeros of the Melnikov function $M(z)$, i.e., they have a finite order of degeneracy.*

Two special cases arise in applications. The first special case is “infinite time dynamics”, i.e., when the (aperiodic) streamfunction ψ is considered a good model for all values of $z = \epsilon t$. If the saddle point $p(z)$ exists for all $z \in (z^-, z^+) = (-\infty, +\infty)$ with its eigenvalues uniformly bounded away from zero, and the right-hand-side of equation (5) is uniformly bounded in z , then a slow manifold P_ϵ exists again for all values of z by a result of Coppel (1978). Furthermore, the usual Melnikov calculation for the intersection of $W^u(P_\epsilon)$ and $W^s(P_\epsilon)$ applies (see, e.g., Balasuriya et al. (1998) for details) and yields the function $M(z)$ as defined in (6).

The second and more important special case is when ψ is T -periodic in ϵt , in which case we can choose $z^+ = z^- + T$, and P_ϵ is in fact a slow periodic orbit. Furthermore, $W^u(P_\epsilon)$ and $W^s(P_\epsilon)$ are invariant manifolds (i.e., not only locally invariant manifolds), and $M(z)$ is periodic in z . As a result, a single transverse zero implies the presence of infinitely many transverse zeros, which in turn implies the presence of a homoclinic tangle for the corresponding Poincaré map. Then the two-dimensional lobes described above are just the usual subjects of lobe dynamics (see, e.g., Wiggins (1992)).

3.1 The eddy-growth criterion for time-periodic flows

If an Eulerian bifurcation occurs in a time-periodic adiabatic problem and the participating eddies satisfy a non-degeneracy condition, then Lagrangian transport must also take place. We formulate this result in the following theorem.

Theorem 3.1 *Consider the streamfunction $\psi(x, y, \epsilon t)$ and assume that it is T -periodic in its last argument. Suppose further that for some fixed $\epsilon > 0$ and for any $t_c \in [0, T)$, there exists a point $p_c(\epsilon t_c) = (x_c(\epsilon t_c), y_c(\epsilon t_c))$ such that a nondegenerate, continuous Eulerian bifurcation occurs at the streamline containing $p_c(\epsilon t_c)$ at time $t = t_c$. If the transport happens via eddy detachment, assume that the area of the detached eddy at some time $t = t^* > t_c$ is bigger than its size at $t = t_c$. Similarly, if the Eulerian bifurcation happens through eddy reattachment, assume that the area of the unattached eddy at some time $t = t^* < t_c$ is bigger than its size at $t = t_c$. Assume further that the function $p_c(\cdot)$ is smooth.*

Then for $\epsilon > 0$ small enough, the Eulerian bifurcation is accompanied by Lagrangian transport of particles which occurs between the interior and the exterior of the region which is encircled by the eddy at $t = t_c$. If $0 \leq z_1 < \dots < z_{2k} < \epsilon T$ are the local extremum points

of the connected eddy area function $A(z)$, then up to an error of order $\mathcal{O}(\epsilon)$, the net Lagrangian flux associated with this transport is given by the formula

$$\text{Flux} = \sum_{i=1}^k |A(z_{2i}) - A(z_{2i-1})|.$$

Proof: Using the notation $z = \epsilon t$, the assumptions of the theorem imply that $\nabla\psi(p_c(z), z) = 0$, and $\frac{\partial^2}{\partial x \partial y} \psi(p_c(z), z)$ is indefinite. This in turn implies the existence of a one-dimensional, normally hyperbolic invariant manifold P_0 for the flow in the $\epsilon = 0$ limit. Since a continuous Eulerian bifurcation always implies the existence of homoclinic or heteroclinic loops attached to $p_c(z)$, P_0 must have a two-dimensional homoclinic or heteroclinic manifold Γ_0 attached to it. For simplicity, we assume that Γ_0 is a homoclinic manifold, since the heteroclinic case can be dealt with similarly. In view of our discussion above, P_0 perturbs into a nearby slow periodic orbit P_ϵ for small $\epsilon > 0$, which admits stable and unstable manifolds. For any $\bar{z} \in [0, T)$, the intersection of $P_\epsilon, W^s(P_\epsilon)$, and $W^u(P_\epsilon)$ with any Poincaré section $\Sigma(\bar{z}) = \{(x, y, z) \mid z = \bar{z}\}$ will yield a hyperbolic fixed point with stable and unstable manifold for the Poincaré map based at $\Sigma(\bar{z})$. (The hyperbolicity of the fixed point follows from the assumption that the Eulerian bifurcation is continuous and nondegenerate.) If the Melnikov has a transverse zero at $z = z_0$, then the stable and unstable manifolds of the fixed point will intersect transversely and hence Lagrangian transport from the interior of $\Gamma_0 \cap \Sigma(\bar{z})$ to its exterior and vice versa. In fact, by the area conservation of the Poincaré map, if $W^s(P_\epsilon) \cap \Sigma(\bar{z})$ and $W^u(P_\epsilon) \cap \Sigma(\bar{z})$ do not coincide, then they must intersect topologically transversely, hence the homoclinic tangle is still developed. In other words, if $M(z)$ is not identically zero, it will always have at least one topologically transverse zero, and Lagrangian transport takes place. Therefore, to prove the first statement of the theorem, we only have to argue that $M(z)$ is not identically zero.

Suppose that the Eulerian bifurcation occurs through eddy detachment. Then for any $t > t_c$, the detaching eddy is a closed streamline which is encircled by the homoclinic loop $\Gamma_0 \cap \Sigma(\epsilon t)$. Therefore, if the area of the eddy at some time $t = t^*$ is greater than the area of the homoclinic loop $\Gamma_0 \cap \Sigma(\epsilon t_c)$ (i.e., the area enclosed by the eddy at the time of its detachment), then we must necessarily have $A(\epsilon t^*) > A(\epsilon t_c)$ (see Fig. 6a). In other words, we have $A(z^*) > A(z_c)$, hence $A(z)$ is not a constant function. Since the function $A(z)$ is at least C^1 , the mean value theorem implies that $dA(\bar{z})/dz \neq 0$ for some $\bar{z} \in (z_c, z^*)$. Then we conclude from formula (6) that $M(z)$ is not identically zero, hence Lagrangian particle transport takes place. A similar argument yields the same result for the case of eddy reattachment (see Fig. 6b). Finally, the statement about the Lagrangian flux through the eddy boundary follows directly from formula (8). \square

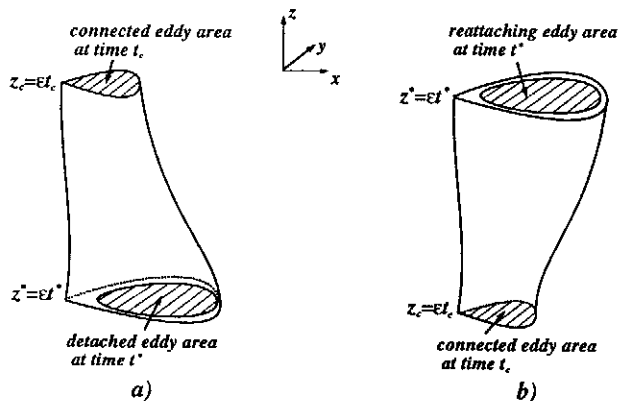


Fig. 6. The geometry behind the proof of the eddy-growth criterion.

Loosely speaking, the above theorem states the following:

In time-periodic, adiabatic flows, growing detached eddies and shrinking reattaching eddies indicate Lagrangian particle transport in directions transverse to the boundaries of the eddies. The flux associated with this transport is given by the difference in eddy areas taken at two adjacent extrema of the connected eddy-area function $A(\epsilon t)$.

It is interesting to note that the shrinkage and growth conditions for the eddy area cannot be relaxed in Theorem 3.1. In other words, if one follows a distinguished set of streamlines, the appearance of an eddy in an Eulerian time series does not immediately imply mixing of Lagrangian particles across separatrices.

To see this, consider the following adiabatic streamfunction

$$\psi(x, y, t) = \left(\frac{1}{2}y^2 - \frac{1}{3}x^3 + x \right) (2 + \sin \epsilon t). \quad (9)$$

The set of streamlines for this function is clearly constant in time, but the value of ψ changes on these streamlines periodically. An easy calculation gives that for $p_c = (x_c, y_c) = (1, 0)$, and for any $t_c \in \mathcal{R}$,

$$\nabla\psi(x_c, y_c, t_c) = 0,$$

and

$$\begin{aligned} E(p_c, t_c) &= \frac{\partial\psi(p_c, t_c)}{\partial t} \frac{\partial^2}{\partial x \partial y} \psi(p_c, t_c) \\ &= (2 + \cos \epsilon t_c) \begin{pmatrix} -2 & 0 \\ 0 & 1 \end{pmatrix}. \end{aligned}$$

Since $E(p_c, t_c)$ is indefinite for all t_c , we conclude that an Eulerian bifurcation occurs for any time $t = t_c$ through

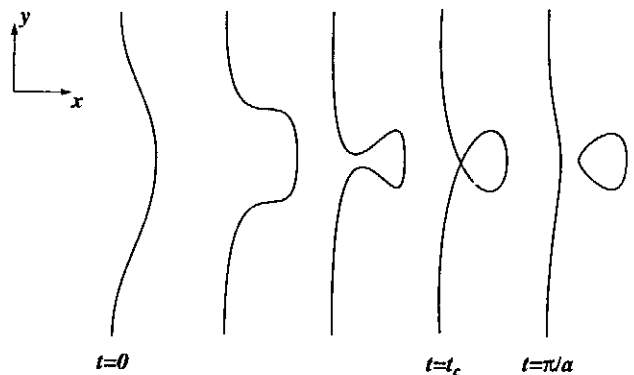


Fig. 7. Periodic eddy detachment in the example.

the streamline that contains the point p_c . (We cannot have an exchange of streamlines since any big enough, fixed ball B containing the point p_c will be intersected in precisely two points by the streamline containing p_c for any time t_c . This follows from the fact that the set of streamlines is fixed and all non-closed streamlines have this intersection property.) The Eulerian bifurcation is manifested by periodic eddy detachment and reattachment (see Fig. 7). The corresponding velocity field is given by

$$\begin{aligned} \dot{x} &= -\frac{\partial\psi}{\partial y} = -(2 + \sin \epsilon t)y, \\ \dot{y} &= \frac{\partial\psi}{\partial x} = (2 + \sin \epsilon t)(1 - x^2). \end{aligned}$$

Introducing the new time $\tau = (2t - (1/\epsilon) \cos \epsilon t)$, we obtain that Lagrangian particle motions obey the equation

$$\begin{aligned} x' &= -y, \\ y' &= 1 - x^2, \end{aligned} \quad (10)$$

where the prime denotes differentiation with respect to τ . This is a one-degree-of-freedom Hamiltonian system, and hence no Lagrangian mixing can occur in the flow governed by the streamfunction (9).

This flow satisfies all the assumptions of Theorem 3.1 except the condition on the change of the eddy area. The reason is that after rescaling time, the scaled system (10) has no explicit time dependence, hence $M(z) = dA(z)/dz \equiv 0$ must hold by integrability. As a result, the detached or reattaching eddy (depending on the sign of ϵ) is always confined to the interior of the region enclosed by the single homoclinic orbit of (10), which bounds the eddy at the time of detachment or reattachment. Consequently, the area of the detaching eddy cannot grow, or the area of the reattaching eddy cannot shrink, so the assumptions of Theorem 3.1 are not satisfied.

4 Mixing in eddy-jet interactions

In this section we study Lagrangian mixing and Eulerian bifurcations in a particular oceanographic flow, namely the kinematic eddy-jet interaction model proposed by Dutkiewicz and Paldor (1994). This model is relatively simple, but appears to capture several important features of the interaction of a Gulf Stream-like jet with an eddy. One of these features found numerically by Dutkiewicz and Paldor is the fact that the presence of an eddy greatly enhances the mixing of Lagrangian particles in the jet. We will explain this numerical observation in terms of Lagrangian transport, whose existence we infer from Eulerian observations. This demonstrates the use of the eddy-growth criterion, as well as that of the classification theorem of Eulerian bifurcations, that we proved in Section 2.

The model flow field is given by the linear superposition of a meandering jet and a simple Gaussian-shaped eddy representing a Gulf Stream ring. The corresponding streamfunction is

$$\psi = \psi_{jet} + \psi_{eddy},$$

where

$$\psi_{jet}(x, y, t) = J \tanh \left\{ \frac{1}{L} (y - A \sin[k(x - ct)]) \right\},$$

$$\psi_{eddy}(x, y, t) = E \exp \left(-\frac{1}{2\sigma^2} [(x - \mu_x)^2 + (y - \mu_y)^2] \right). \quad (11)$$

The parameters in the problem are the maximum jet velocity J , the jet width L , the meander speed c , the meander wavelength k , the meander amplitude A , the eddy size σ , and the eddy center coordinates (μ_x, μ_y) . The parameters are chosen to match observations of the Gulf Stream and its eddy field. In particular, we have the parameter values

$$J = 4.5 \text{ km}^2/\text{min}, \quad L = 50 \text{ km}, \quad c = 0.007 \text{ km}/\text{min},$$

$$k = 0.0157 \text{ 1}/\text{km}, \quad A = 60 \text{ km}, \quad \sigma^2 = 625 \text{ km}^2,$$

$$(\mu_x, \mu_y) = (400 \text{ km}, -100 \text{ km}).$$

We note that the ratio of the propagation speed of the jet meander to typical particle speeds in the interior of the jet is small. As a result, we can define the adiabatic parameter

$$\epsilon = \frac{u_{meander}}{u_{particle}} \approx \frac{10 \text{ km}/\text{day}}{150 \text{ cm}/\text{s}} = \mathcal{O}(0.1) \quad (12)$$

which, while not infinitesimally small, will turn out to be adequate for relating Eulerian bifurcations to Lagrangian transport via the eddy growth criterion.

First, we want to determine the time t_c and the location $p_c = (x_c, y_c)$ of continuous Eulerian bifurcations.

To verify the conditions of Theorem 2.1, we have to find the zeros of the equation $\nabla\psi(x_c, y_c, t_c) = 0$, and study the eigenvalue configuration of the matrix $E(p_c(t_c), t_c)$. Since the former equation is transcendental in this example, we can only find the curve of zeros $p_c(t_c)$ numerically. This amounts to selecting a time slice t_c and searching for a fixed point (x_c, y_c) of the time-independent flow generated by streamfunction $\psi(x, y, t_c)$. From (4) and (11) we can compute the matrix $E(p_c, t_c)$ and its eigenvalues numerically. The Eulerian bifurcation curves $p_c(t_c)$ and the definiteness properties of $E(p_c(t_c), t_c)$ along the curves are shown in Fig. 8 for two different parameter values. These parameter values are taken to illustrate the two qualitatively different eddy-jet interactions: the strong and the weak eddy case.

For the strong eddy case, a pair of critical curves $p_c(t_c)$ exists for all values of t_c . The larger curve traces the hyperbolic saddle point which indicates eddy reattachment initially as the jet meander approaches the eddy, then eddy detachment as the meander moves away. The smaller curve tracks the continuous eddy creation/disappearance that occurs at the center of the homoclinic loop.

In the weak eddy case, there are no critical points in any of the time slices initially. At some point, as the jet meander moves far enough away from the eddy center, a pair of critical points are created, one corresponding to the birth of a saddle, the other to a center. These two points then move on a curve in the phase plane until the next jet meander approaches and the two critical points coalesce in a Hamiltonian saddle-node bifurcation for the Hamiltonian $\psi(x, y; t_c)$. In the strong eddy case, a stagnation point p_c exists for all times, while in the weak eddy case the curve $p_c(t_c)$ is only defined for a range of t_c values which is smaller than the period of the streamfunction.

In conclusion, Fig. 8 shows that *continuous Eulerian bifurcations occur for all times t_c in the strong eddy case, and for a range of times t_c in the weak eddy case*. In Figs. 9 and 10 we show contour plots of the combined streamfunction ψ at three different times for $E = 4.5$ (strong eddy) and for $E = 3.0$ (weak eddy).

For the strong eddy case, a closed, homoclinic loop in the dynamics generated by the Hamiltonian $\psi(x, y, t_0)$ exists for all times t_0 in the period, even when the eddy and the jet are at the point of closest proximity. In the weak eddy case, the closed streamline loop, i.e., the homoclinic orbit of $\psi(x, y, t_0)$ disappears for times t_0 when the jet meander approaches the eddy too closely (see Fig. 10).

Having obtained a fairly complete understanding of the Eulerian properties of the eddy-jet interaction model, we now would like to use our ‘‘Eulerian observations’’ to study Lagrangian particle transport in the problem. To apply our eddy-growth criterion (Theorem 3.1), we note that in both the strong and the weak eddy cases, detaching eddies grow and reattaching eddies shrink. This

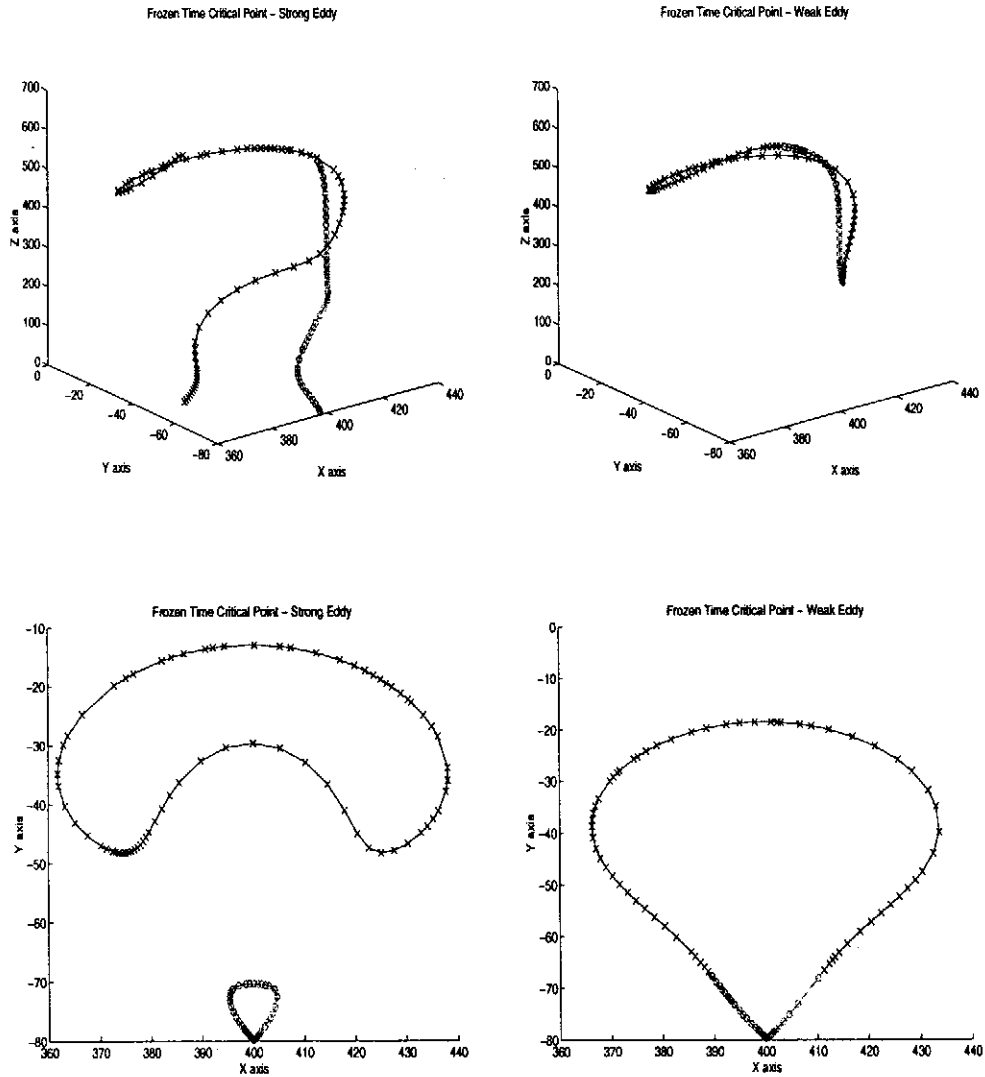


Fig. 8. Eulerian bifurcation curves for both strong and weak eddy parameters. In the figures \times indicates that $E(p_c, t_c)$ is indefinite, and hence eddy detachment or reattachment occurs at p_c . Similarly, \circ indicates that $E(p_c, t_c)$ is definite, thus eddy creation or disappearance takes place.

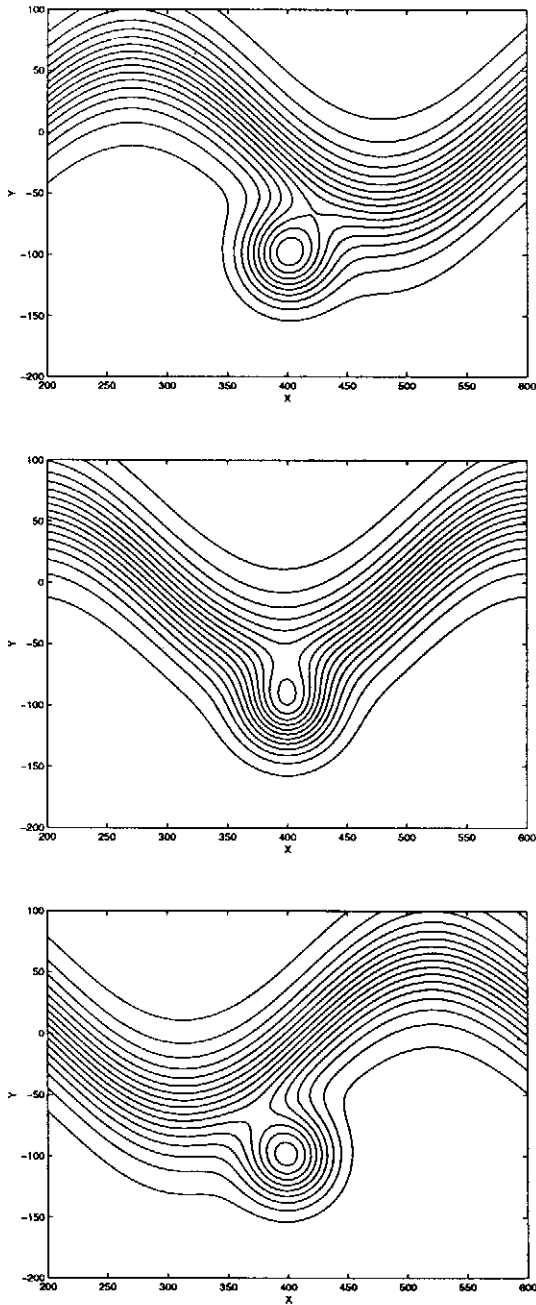


Fig. 9. Streamfunction contours for the strong-eddy case. Snapshots taken at times $t = 0$, top, $t = 0.16T$, middle; $t = 0.32T$, bottom. Spatial coordinates in km , contour spacing $0.5km^2/min$.

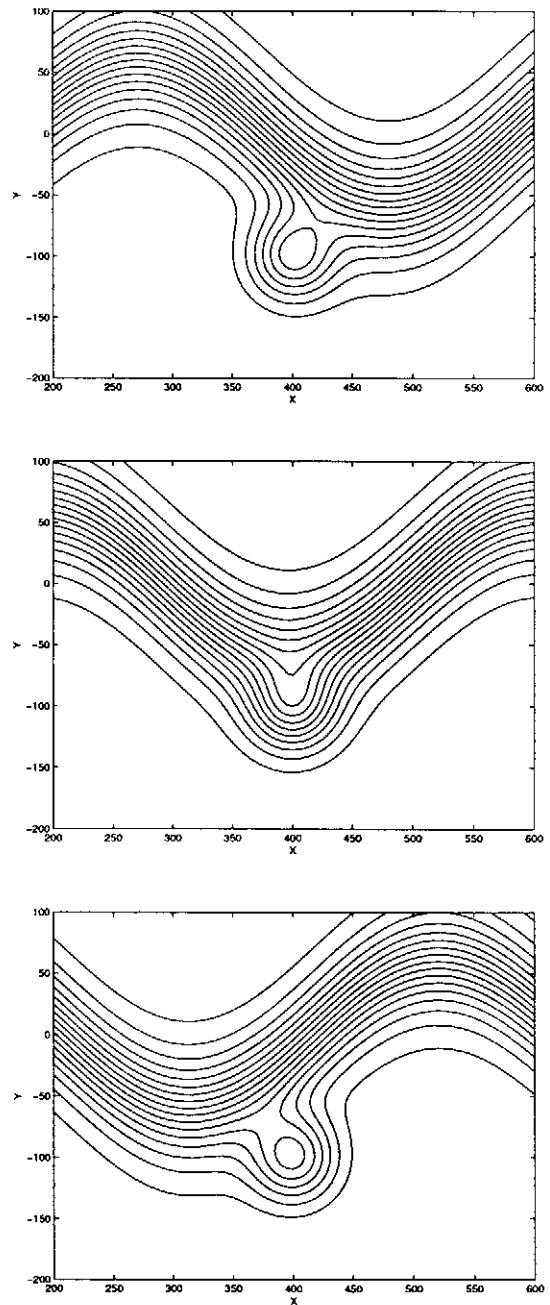


Fig. 10. Streamfunction contours for the weak-eddy case. Snapshots taken at times $t = 0$, top, $t = 0.16T$, middle; $t = 0.32T$, bottom. Spatial coordinates in km , contour spacing $0.5km^2/min$.

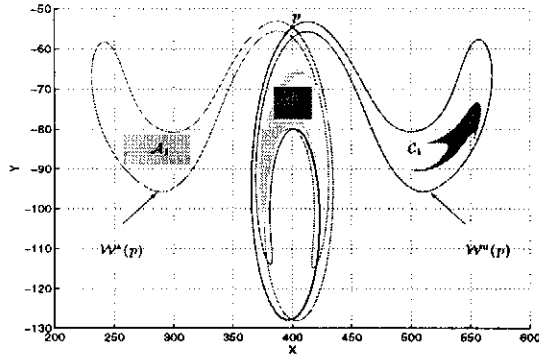


Fig. 11. Lagrangian transport in the eddy-jet interaction model.

can be seen from the Eulerian slices given in Figs. 9 and 10. Therefore, by Theorem 3.1, for $\epsilon > 0$ sufficiently small, Lagrangian transport of particles occurs in the strong eddy case in directions transverse to the eddy boundaries. We cannot reach a similar conclusion for the weak eddy case, since we do not have the existence of a saddle-type stagnation point for all times, hence the conditions of Theorem 3.1 are not satisfied.

Since our adiabatic parameter ϵ is not infinitesimally small, a numerical verification of Lagrangian transport is needed for the physically meaningful value of ϵ given in (12). In order to actually demonstrate Lagrangian transport in the strong eddy case, we construct a Poincaré map of the corresponding time-periodic flow. We generate this map by strobing at the time when the fixed time homoclinic loop is the largest. Fixing a time slice $t = t_c$ and using the techniques described in Miller et al. (1997), we can locate the hyperbolic fixed point p_c of the Poincaré map based at $t = t_c$. By elementary perturbation theory, the fixed point p_c must be $\mathcal{O}(\epsilon)$ -close to the stagnation point $p_c(t_c)$ with local stable and unstable manifolds $W_{loc}^s(p_c)$ and $W_{loc}^u(p_c)$. These local manifolds are C^1 $\mathcal{O}(\epsilon)$ -close to the homoclinic loop of the Hamiltonian $\psi(x, y, t_c)$. Using software tools developed by Miller et al. (1997), we can find the global stable and unstable manifolds $W^s(p_c)$ and $W^u(p_c)$, as shown in Fig. 11.

Note that $W^s(p)$ and $W^u(p)$ intersect each other transversely, which implies the existence of Lagrangian particle transport via the lobes of the resulting homoclinic tangle. To illustrate the mixing induced by the presence of lobes, we seeded the primary lobe with a rectangle of initial conditions and iterated the Poincaré map in forward time. Only those particles initially located in the area marked $A1$ (see Fig. 11) are mapped into the recirculating eddy region in a single iterate. Similarly,

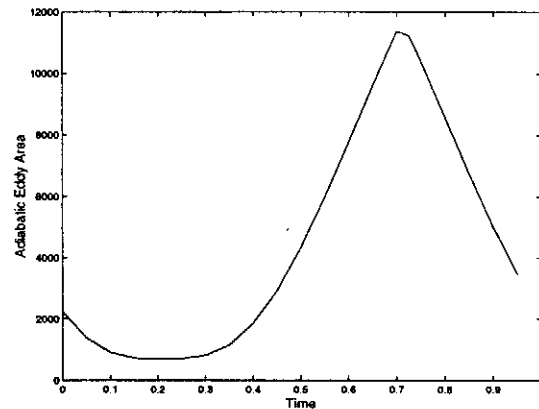


Fig. 12. Area of the bounded eddy region as a function of time. Areas given in km^2 , time in fractions of a period.

particles originating in region $B1$, inside the eddy, are swept into the jet in one iteration of the map.

We note that the lobes computed for this case have the characteristic features that are typical of adiabatic Hamiltonian systems (Kaper and Wiggins (1991), Kaper and Kovačič (1994), etc.). In particular, the lobe areas are $\mathcal{O}(1)$ quantities while their widths are $\mathcal{O}(\epsilon)$, which results in highly elongated and twisted mixing regions. The physical implications of adiabaticity in this class of oceanographic flows will be treated in detail elsewhere.

In order to directly estimate the Lagrangian particle flux between the eddy and the jet, we first calculate the area of the fixed time, bounding homoclinic orbit. The resulting areas for the strong eddy case are shown in Fig. 12 over the course of a single time period, $t \in (0, T = 2\pi/(kc))$. We note, in this case where we are dealing with the streamfunction directly, the bounding curve is easily found. Once the location of the fixed time stagnation point is known, the homoclinic orbit is easily constructed by initializing a trajectory nearby and following the closed loop back to the initial conditions. For more general situations, the location of the Eulerian bifurcation point provides a critical value for the Eulerian field of interest. One can then examine the level curves at this critical value to determine the area of the bounded region.

The area curve for the strong eddy case shows two extrema and thus, from Eq. (7), two zeros of the Melnikov function M . The time derivative, measuring the instantaneous particle flux, is plotted in Fig. 13. There is a short period of time initially, where the flux is negative; particles in the eddy are transported into the jet. Following this, the eddy grows, entraining jet fluid until, at time $t \approx 0.7T$, the eddy reaches a maximum size and

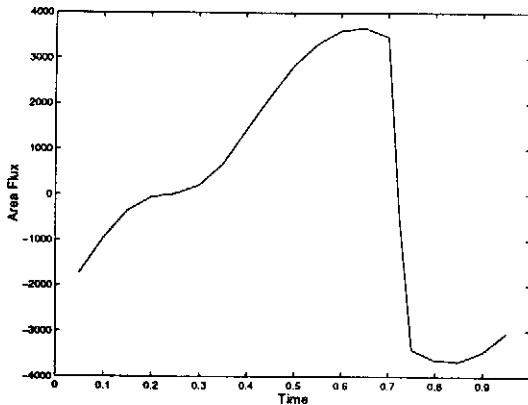


Fig. 13. Melnikov function, $M(t)$ over a single period. M given in $\frac{km^2}{T}$, where T is the time period. The time is in fractions of a period.

there is a rapid changeover in the direction of particle transport. The cycle then repeats itself periodically.

The dimensional value of the flux depends on the choice of meander speed c . For the values given above, the period is,

$$T = \frac{2\pi}{kc} \approx 40 \text{ days}.$$

Figure 12 shows the total growth in eddy area is approximately 10,000 square kilometers in a time of order $T/2$. Assuming the kinematic model applies in a 500 meter deep surface layer, the average volume flux into the eddy over the half cycle is of order 2.8 Sv, agreeing reasonably well with Gulf Stream observations.

5 Conclusions

In this paper we developed a geometric concept of Eulerian bifurcations, i.e., qualitative changes in extended structures in two-dimensional, time dependent flows. Such structures are typically defined through the streamfunction or some other passive scalar associated with the flow. We define an Eulerian bifurcation as a change in the topology of these structures. Such a change can only occur at stagnation points of the flow, i.e., at points $p_c = (x_c, y_c)$ and at some time t_c such that $\nabla\psi(x_c, y_c, t_c) = 0$. Our classification theorem (Theorem 2.1) states that in the generic case, an Eulerian bifurcation manifests itself in eddy creation, disappearance, detachment, or reattachment. These cases can be determined completely from the eigenvalue configuration of the matrix $E(p_c, t_c)$ defined in (4). We note that recent work has shown the existence of a streamfunction in non-divergent, three dimensional flows (see Mezić and Wiggins (1994) and

Haller and Mezić (1996)). Although more difficult, a similar classification of the Eulerian bifurcations would prove a useful tool for understanding the much richer 3D topology and mixing processes.

In the case of adiabatic flows with periodic time dependence, we established a direct correspondence between Eulerian bifurcations and Lagrangian transport. The eddy-growth criterion (Theorem 3.1) guarantees the existence of Lagrangian transport based on observations of eddies and their deformation. This criterion gives an efficient visual tool to study nearly periodic experimental data sets. If the experimental flow is sufficiently close to a periodic field and satisfies the eddy-growth criterion, then the periodic limit will also satisfy the criterion, and hence exhibit Lagrangian transport. But this transport is due to the (topologically) transverse intersection of stable and unstable manifolds, therefore it persists for the nearby aperiodic flow studied originally.

The eddy-growth criterion is equally useful for nearly-periodic, numerically generated vector fields with slow time dependence. A dynamical systems-type analysis of such problems is very difficult, since even few iterations of an approximate Poincaré map require the solution of the vector field on times scales of order $\mathcal{O}(1/\epsilon)$. Since the vector field is already just an approximation of the true velocity field, the long-term integration of initial conditions leads to error accumulation. These errors are particularly undesirable in the computation of adiabatic lobes, which exhibit very intense stretching and folding. For all these reasons, the Eulerian observations of eddy dynamics required for the application of the eddy-growth criterion are substantially easier to obtain than long-time Lagrangian information derived from the direct integration of the velocity field.

The main results were demonstrated in a study of an eddy-jet interaction model of Dutkiewicz and Paldor. Using the corresponding streamfunction, the location, time, and type of Eulerian bifurcations in the problem were predicted. We also showed that the conditions of the eddy-growth criterion are satisfied for the case of a strong eddy, and hence Lagrangian transport occurs in the problem in the case when the velocity of the jet meander is sufficiently small compared to typical particle speeds in the jet. We verified the existence of Lagrangian transport numerically for a fixed set of parameter values by locating stable and unstable manifolds for the corresponding Poincaré map.

An interesting open question is the treatment of “transient” stagnation points, i.e., stagnation points that only exist for a limited amount of time, just like those in the weak eddy case that we considered in Section 4. Such stagnation points do not necessarily imply the existence of a hyperbolic fixed point for the period- T map, yet they seem to induce substantial mixing and transient hyperbolic behavior. The organization of particle trajectories by transient hyperbolicity is an established feature of particle dispersion in two-dimensional turbulence

(Provenzale et al. (1995) Elhmaïdi et al. (1993)). Such flows are dominated by the presence of coherent structures which, while highly aperiodic in time, are adiabatic in nature. The organizing vortices evolve on time scales slower than the particle dynamics. The structures are long lived, existing for many eddy turnover times.

To approach the aperiodic, 'transient eddy' case, one needs new and more sophisticated mathematical methods. In a companion paper Haller and Poje (1997), we lay the mathematical groundwork for a finite time mixing theory. Similar to the approach of the present paper, we identify potential mixing regions by finding *transient* stagnation points of the fixed time, Eulerian flow field. We then give a set of explicit conditions under which the full flow admits nearby hyperbolic trajectories. The stable and unstable manifolds of such solutions are only unique up to exponentially small errors, which, however, is more than sufficient in the analysis of experimental or numerical data sets. Unlike earlier mixing analyses, this theory does not rely on the presence of infinitesimally small perturbation parameters, and hence can be applied directly to observational data sets.

Acknowledgment

We would like to thank Stephanie Dutkiewicz and Pat Miller for useful discussions and explanations of their work. We are also grateful to Chris Jones for suggestions and clarifications of questions in adiabatic transport. This work was supported by ONR Grant No. N00014-93-I-0691. G.H. partially supported by NSF Grant No. DMS-95-1239 and a Sloan Fellowship.

References

- Aref, H., Stirring by chaotic advection, *J. Fluid Mech.*, **143**, 1-21, 1984.
- Balauriya, H. S., Jones, C.K.R.T. and Sandstede, B., Viscous perturbations of vorticity-conserving flows and separatrix splitting. *Nonlinearity*, **11**, 47-77, 1998.
- Coppel, W.A., *Dichotomies in Stability Theory*, Lect. Notes in Math. 629, Springer-Verlag, New York, 1978.
- Dutkiewicz, S. and Paldor, N., On the mixing enhancement in a meandering jet due to the interaction with an eddy, *J. Phys. Oceanogr.* **24**, 2418-2423, 1994.
- Elhmaïdi, D., Provenzale, A., Babiano, A., Elementary topology of two-dimensional turbulence from a Lagrangian viewpoint and single-particle dispersion, *J. Fluid Mech.*, **257**, 533-558, 1993.
- Feliks, Y. and Ghil, M., Mixed barotropic-baroclinic eddies growing on an eastward midlatitude jet, *Geophys. Astrophys. Fluid Dynamics* **32**, 1-35, 1996.
- Fenichel, N., Persistence and smoothness for invariant manifolds for flows, *Indiana Univ. Math. J.* **21**, 193-225, 1971.
- Haller, G., and Mezić, I., Reduction of three dimensional volume preserving flows with symmetry, *Nonlinearity*, **11**, 319-339, 1998.
- Haller, G., and Poje, A.C., Finite time transport in aperiodic flows, *Physica D*, (1998), to appear.
- Holdzkom, J.J., Hooker, S.B. and Kirwan, A.D., A comparison of a hydrodynamic lens model to observations of a warm core ring, *J. Geophysical Res.*, **100**, 15,889-15,897, 1995.
- Kaper, T. J. and Wiggins, S., Lobe area in adiabatic Hamiltonian systems, *Physica D* **51**, 205-212, 1991.
- Kaper, T.J. and Kovačić, G., A geometric criterion for adiabatic chaos, *J. Math. Phys.* **35/3**, 1202-1218, 1994.
- Lozier M.S., Pratt L.J., Rogerson A.M., & Miller P.D., Exchange geometry revealed by float trajectories in the Gulf Stream. *J. Phys. Oceanogr.*, **27**, 2327-2341, 1997.
- MacKay, R.S., Meiss, J.D., Percival, I.C., Transport in Hamiltonian systems, *Physica D* **13**, 55-81, 1984.
- Mezić, I. and Wiggins, S., On the integrability and perturbation of three dimensional fluid flows with symmetry, *Journal of Nonlinear Science*, **4**, 157-194, 1994.
- Miller, P.D., Jones, C.K.R.T., Rogerson, A.M., and Pratt, L.J., Quantifying transport in numerically generated velocity fields, *Physica D*, **110**, 105-122, 1997.
- Provenzale, A., Babiano, A., and Villone, B., Single-particle trajectories in two-dimensional turbulence, *Chaos, Solitons & Fractals*, **5**, 2055-2071, 1995.
- Pratt, L.J. and Stern, M.E., Dynamics of potential vorticity fronts and eddy detachment, *J. Phys. Oceanogr.* **16**, 1101-1120, 1986.
- Ridderinkhof H. and Zimmerman, J.T.F., Chaotic stirring in a tidal system, *Science* **258**, 1107-1111, 1992.
- Rom-Kedar, V., Leonard, A., and Wiggins, S., An analytical study of transport, mixing, and chaos in an unsteady vortical flow, *J. Fluid. Mech.* **214**, 347-394, 1990.
- Samelson R.M. Fluid exchange across a meandering jet, *J. Phys. Oceanography* **21**, 431-440, 1995.
- Song, T., Rossby, H.T. Carter, E., Lagrangian studies of fluid exchange between the Gulf Stream and surrounding waters. *J. Phys. Oceanogr.*, **25**, 46-63, 1995.
- Wiggins, S., Homoclinic orbits in slowly varying oscillators, *SIAM J. Math. Anal.* **18**, 612-629, 1987.
- Wiggins, S., *Chaotic Transport in Dynamical Systems*, Springer, New York, 1992.
- Wray, A.A., and Hunt, J.C.R., Algorithms for classification of turbulent structures, in *Topological Fluid Mechanics*, Moffatt, H.K., and Tsinober, A. (eds.), Cambridge University Press, Cambridge, 1990.